DOI: 10.1002/chem.201001653

Hydrogen Bonding Versus van der Waals Interactions: Competitive Influence of Noncovalent Interactions on 2D Self-Assembly at the Liquid–Solid Interface

Kunal S. Mali,[a] Kathleen Lava,[b] Koen Binnemans,[b] and Steven De Feyter*[a]

Abstract: The structures of the self-assembled monolayers of various 4-alkoxybenzoic acids physisorbed at the liquid–solid interface were established by employing scanning tunnelling microscopy (STM). This study has been essentially undertaken to explore the competitive influence of van der Waals and hydrogen-bonding interactions on the process of two-dimensional self-assembly. These acid derivatives form hydrogen-bonded dimers as expected; however, the dimers organise themselves in the form of relatively complex lamellae. The characteristic feature of these lamellae is the presence of regular discommensurations or kinks along the lamella propagation direction. The formation of kinked lamellae is discussed in light of the registry mechanism of the alkyl chains with the underlying graphite substrate. The location of the kinks along a lamella depends on the number (odd or even) of carbon atoms in the alkyl chain. This result indicates that concerted van der Waals interactions of the alkyl chain units introduce the odd/even chain-length effect on the surface-assembled supramolecular patterns. The odd/even effects are retained even upon complexation with a hydrogen-bond acceptor. However, as the solvent is changed from 1-phenyloctane to 1-octanoic acid, the kinked lamellae as well as the odd/even effects disappear. This solvent-induced convergence of supramolecular patterns is attained by means of co-crystallisation of octanoic acid molecules in the 2D crystal lattice, which is evident from high-resolution STM images. The solvent co-adsorption phenomenon is discussed in terms of competing van der Waals and hydrogen-bonding interactions.

Keywords: liquid–solid interfaces · noncovalent interactions · scanning probe microscopy · self-assembly · solvent effects

Introduction

The phenomenon of molecular self-assembly is ubiquitous in nature and can be observed in many chemical, physical and biological systems.[1] Self-assembly has been recognised as one of the powerful means of fabricating functional nanomaterials by employing well-designed molecules as building blocks.[2,3] Thus, understanding the organisation of molecules on solid surfaces is fundamental for the realisation and ensuing development of surface-supported molecular nanostructures and nanodevices.[2–20] Scanning tunnelling microscopy (STM) is one of the preferred techniques for investigating the ordering and properties of self-assembled layers—in general, monolayers, both under ultrahigh vacuum conditions[21]—as well as the liquid–solid[22] or air–solid interface. STM offers a unique possibility of not only submolecular visualisation but also manipulation of these adsorbed nanostructures. Successful formation and subsequent visualisation of a monolayer necessitates a delicate balance between various attractive and repulsive forces. In general, relatively weak intermolecular interactions such as van der Waals, hydrogen-bonding, dipole–dipole interactions and metal coordination have been exploited to form well-defined two-dimensional (2D) monolayers on surfaces.[23]

Supramolecular surface motifs based on hydrogen-bonding interactions are one of the most frequently encountered self-assembled structures due to the relatively strong, selective and directional nature of hydrogen bonds. Carboxyl

[a] Dr. K. S. Mali, Prof. S. De Feyter
Division of Molecular and Nanomaterials
Department of Chemistry and
INPAC-Institute of Nanoscale Physics and Chemistry
Katholieke Universiteit Leuven, Celestijnenlaan 200F
P.O. Box 2404, 3001 Leuven (Belgium)
Fax: (+32) 16-327990
E-mail: Steven.DeFeyter@chem.kuleuven.be

[b] K. Lava, Prof. K. Binnemans
Laboratory of Coordination Chemistry
Department of Chemistry
Katholieke Universiteit Leuven, Celestijnenlaan 200F
P.O. Box 2404, 3001 Leuven (Belgium)

Supporting information for this article is available on the WWW under http://dx.doi.org/10.1002/chem.201001653.

functional groups are probably the most widely exploited synthons for hydrogen-bonded motifs since they are endowed with a very interesting and unique "self-complementary" hydrogen-bonding ability. Thus, they exhibit dual nature on account of the presence of the oxygen atom of the carbonyl group, which acts as a hydrogen-bond acceptor, whereas the hydroxyl group acts as a hydrogen-bond donor. Consequently, two carboxylic groups can form a cyclic dimer interconnected by two equivalent hydrogen bonds. The role of hydrogen bonding in the process of 2D crystallisation is perfectly illustrated by the behaviour of benzene carboxylic acids, which have proven to be excellent examples of "two-dimensional tectons" and form 2D supramolecular networks by means of hydrogen-bonding interactions. Phthalic acid, isophthalic acid (ISA), terephthalic acid (TA) and trimesic acid (TMA) all contain carboxylic acid functions that can act as hydrogen-bond donors and acceptors simultaneously. It has been confirmed by now that phthalic acid cannot form extended hydrogen-bonded arrays, whereas TA and ISA form dense monolayers in which the molecular self-assembly is dominated by hydrogen-bonding interactions.[24] The self-assembly of TMA,[25–29] on the other hand, has served as a pioneering example of a nanoporous self-assembled network that is formed both in ultrahigh vacuum (UHV) conditions[25] as well as at the liquid–solid interface.[26] The well-defined and robust nanoporous networks formed by TMA have been extensively utilised to host a variety of guests.[27,28] Furthermore, TMA has proven to be a suitable building block for a variety of multicomponent surface architectures.[27–29]

In contrast to hydrogen bonds, van der Waals interactions between alkyl chains are neither strong enough nor directional in nature. The interdigitation as well as epitaxial adsorption of alkyl chains on the surface of graphite, however, which is mainly governed by van der Waals interactions, imparts some kind of unconventional directionality to the molecular self-assembly. Besides this, although the typical energy of van der Waals interactions is less than 5 $kJ\,mol^{-1}$, collectively these interactions can compete with the hydrogen-bonding interactions. (The calculated interaction energy for interdigitated alkyl chains is 7.88×10^{-21} J per methylene group if the alkyl chain is flanked by other alkyl chains on both sides.[30]) Typically, the energy of a twofold O–H···O= hydrogen bond between two carboxylic acids is approximately $-60\,kJ\,mol^{-1}$,[31] whereas the adsorption energy of methane on the surface of graphite is $-12.2\,kJ\,mol^{-1}$[32] and it increases proportionately with the length of the alkane with an increase of around 12.1 $kJ\,mol^{-1}$ for each methylene unit.[33] The influence of alkyl substituents on the 2D self-assembly of alkoxylated isophthalic acid molecules has also been investigated in the recent past. It was demonstrated that the 2D supramolecular ordering can be controlled by varying the location and nature of alkyl substituents on the aromatic core in combination with the intrinsic hydrogen-bonding properties of the ISA units.[34,35]

Apart from the functionality of the building blocks, the fate of a 2D supramolecular pattern also depends critically on the nature of solvent and the substrate used. Since it is one of the elegant ways to control and manipulate the self-assembly, quite a few studies are available that deal with the influence of solvent on the pattern formation at the liquid–solid interface.[36–48] However, despite the multitude of examples already investigated, it is still difficult to generalise the role of solvent molecules in the process of self-assembly. Co-adsorption of solvent molecules has been observed in several instances, which is partly due to enhanced substrate–solvent interactions.[37,38] Solvent co-adsorption is also governed by the size and shape of the solvent molecules[40] as well as the mode of interaction (for example, hydrogen-bonding or van der Waals interactions) of the solvent molecules with the adsorbate.[35] The solvent also enables adsorption–desorption dynamics, thereby affecting the mobility of the molecules at the liquid–solid interface.[43] The two solvent parameters that possibly govern this dynamics are solvation energy and solvent viscosity.[44,45] The solvent-induced polymorphism, effect of co-adsorption as well as the solvent effects on chirality and electronic structures have been summarised recently.[48]

Although the molecules that possess two or three carboxylic groups have been explored extensively, investigations that deal with simple monocarboxylic acids such as 4-alkoxybenzoic acid (4-ABAs) derivatives are astoundingly sparse. In fact, to the best of our knowledge, the self-assembly of 4-ABAs has not been explored systematically except for a very recent report by Matzger et al.[49] In this report, they investigated the self-assembly of 4-ABAs as well as the corresponding amides. The acid derivatives formed a compact lamellar phase irrespective of the number of carbon atoms in the alkyl chain. On the other hand, the amide derivatives gave rise to highly symmetric nanoporous networks that contained rhombic voids. The absence of a porous phase in the acids was attributed to the geometrical difference in the hydrogen-bonding ability of amide and acid molecules.[49]

The principles of molecular self-assembly have been exploited for more than a decade to fabricate new materials with unprecedented properties.[2–20] However, the ability to systematically tailor the self-assembled patterns is only slowly evolving. This is due to the fact that the outcome of a 2D supramolecular pattern is rarely encoded by the molecular building block and it strongly depends on, among other factors, various noncovalent interactions. Thus, the understanding and subsequent control of noncovalent interactions assumes special importance in the quest for novel supramolecular nanostructures. In this contribution, we have systematically investigated the 2D self-assembly of various 4-ABAs that possess different alkyl substitution at the liquid–HOPG (highly oriented pyrolytic graphite) interface, which is virtually an unexplored system. The main goal of this investigation is to explore the competitive influence of hydrogen-bonding and van der Waals interactions on the process of 2D self-assembly at the liquid–solid interface. To this end, we first look into the details of the self-assembly process, which is quite unique for this class of molecules. Complexa-

tion studies were undertaken with an intent to modulate the supramolecular assembly by introducing a hydrogen-bond-accepting component. The interplay between van der Waals and hydrogen-bonding interactions was also probed at the level of solvent. Studies carried out in different solvents highlight the importance of balance between noncovalent interactions such as hydrogen-bonding and van der Waals interactions on the process of 2D self-assembly.

Results and Discussion

Two-dimensional supramolecular patterns formed by 4-ABAs: The peculiarity of the 2D self-assembly of 4-ABAs, particularly in comparison with that of di- or tricarboxylic acids such as TA, ISA and TMA, is that one molecule of acid can be involved in only one intermolecular hydrogen-bonding motif.[50] This implies that once these dimers are formed, they can be considered to be individual building blocks of self-assembly. Deposition of 4-ABAs from a solution of 1-phenyloctane on the surface of HOPG leads to spontaneous formation of stable physisorbed monolayers. Figure 1a displays a large-scale STM image of 4-icosyloxybenzoic acid (**4-OC$_{20}$BA**) at the 1-phenyloctane–HOPG interface. The monolayer emerges with a lamellar feature with clear distinction between regions of bright and dark contrast. On account of the higher electron density of the aromatic core, the bright regions can be attributed to the phenyl rings of the acid molecules, whereas the regions of darker contrast correspond to the alkoxy chains. A submolecularly resolved image of the same derivative displayed in Figure 1b allows us to discern some of the minute features of this lamellar structure. The bright rings in Figure 1b always show up in pairs, which is a strong indication that these molecules form hydrogen-bonded dimers as expected. The width of the lamella is (5.7 ± 0.1) nm and it is indicated as ΔL. In contrast to what has been observed for isophthalic acid derivatives at the HOPG–liquid interface,[34,35] these dimers form tilted rows instead of straight rows. However, the most characteristic feature of these lamellae is the presence of regular discommensurations or kinks along the lamella propagation direction. The kinks appear after every three dimers are formed (that is, every (1.8 ± 0.1) nm) and the next three dimers are shifted with respect to the previous triplet of dimers. As a consequence of these regular discommensurations along the lamella axis, the monolayer structure appears to be relatively more complex compared to the one formed by alkylated ISA molecules. The alkoxy chains in Figure 1b are particularly well resolved. They are fully extended, closely packed and are aligned along one of the symmetry axes of the underlying graphite lattice. The orientation of the alkyl chains with respect to the lamella axis is $(57.6\pm1.2)°$ and the lamellae in turn make an angle of $(5.4\pm1.0)°$ with one of the graphite symmetry axes. The alkyl chains in the neighbouring lamellae are arranged in a tail-to-tail fashion and there is no alkyl chain interdigitation within the adjacent lamellae. The distance between the alkyl chains of two adjacent molecules within the same lamella and perpendicular to the alkyl-chain orientation is (0.49 ± 0.02) nm, which is slightly higher than the distance observed between long-chain alkanes (≈0.45 nm) adsorbed on graphite.[51] The intermolecular distance within the same lamella and along the lamella propagation direction is (0.60 ± 0.02) nm, which correlates well with the periodicity of the kinks.

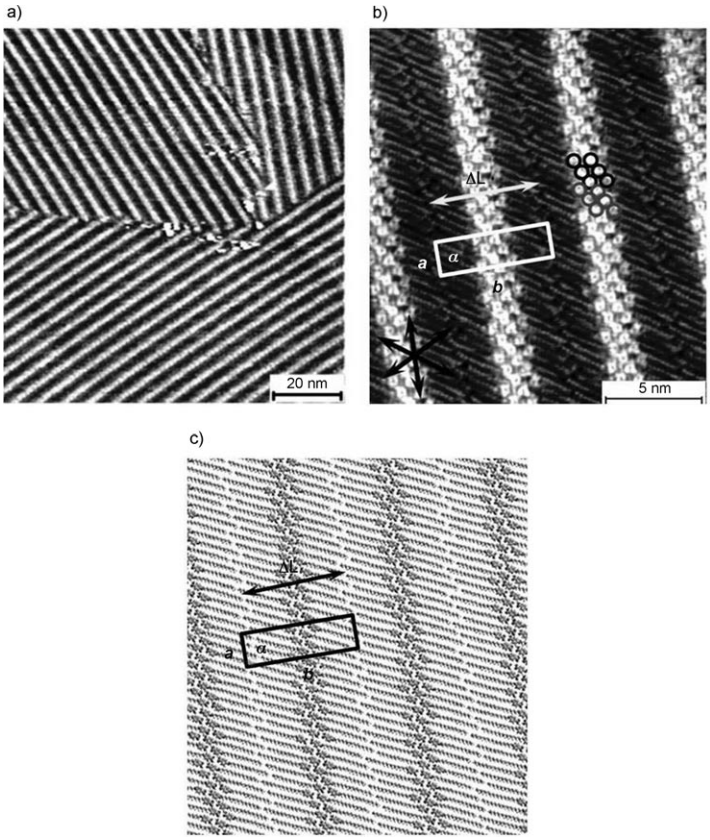

Figure 1. a) Large-scale and b) high-resolution STM images of **4-OC$_{20}$BA** physisorbed at the 1-phenyloctane/HOPG interface. The bright ringlike features in (b) are attributed to the phenyl rings of the acid molecules, whereas striped features with a darker contrast represent the alkyl chains of the molecules. The width of the lamella is indicated as ΔL. The unit-cell parameters are as follows: $a=(1.79\pm0.03)$ nm, $b=(5.73\pm0.04)$ nm and $\alpha=(87.9\pm0.5)°$ (plane group $p2$). The main symmetry axes of the underlying graphite substrate are indicated in the lower left corner of the STM image. Imaging conditions: $I_t=0.25$ nA, $V_{bias}=-0.78$ V. c) Tentative model depicting the molecular arrangement.

Having resolved the microscopic features of the monolayer, we now focus on establishing the rationale behind the emergence of the kinked lamellae. Figure 2, displays a rather rough schematic of the expected (Figure 2a) and observed (Figure 2b) molecular arrangement. On the basis of hydrogen-bonding interactions and substitution pattern, one anticipates these molecules to form dimers that are expected to organise in a continuous lamellar structure as shown in Figure 2a. However, we observe periodic dislocations in the crystal lattice along the lamella propagation direction as shown in Figure 2b. Examples of similar discontinuous lamellar structures can be traced back to the early STM inves-

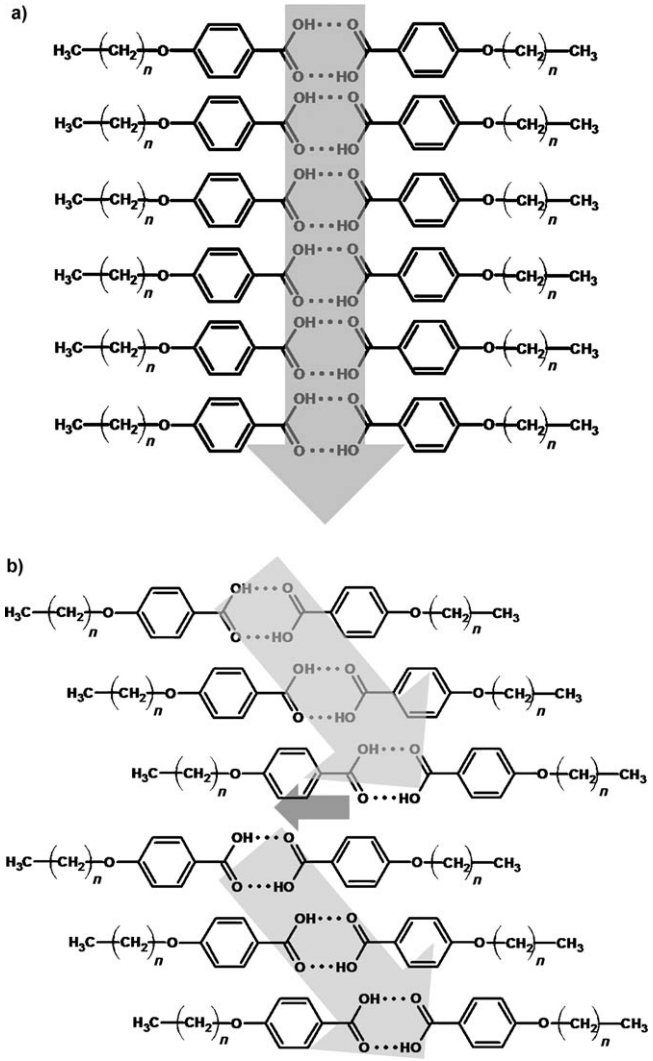

Figure 2. Schematic showing a) the expected and b) observed self-assembled structures of 4-alkoxybenzoic acids. Instead of forming continuous rows as displayed in (a), the molecules form discontinuous rows as shown in (b). In this type of arrangement, after every three dimers the molecules shift with respect to the previous triplet of dimers, thus giving rise to periodic dislocations or kinks along the lamella axis.

tigations on alkylated cyanobiphenyl molecules. The monolayers formed by these liquid-crystalline molecules on atomically flat conductive surfaces such as HOPG[42–60] and/or MoS_2[54,59,60] were the centre of focus in many of the early STM investigations. Periodic dislocations observed in the crystal structures were explained on the basis of strong molecule–substrate interactions and the registry mechanism of the alkyl chains with the underlying substrate.[55] Thus, on the basis of these literature reports, we can explain the discontinuous lamellar features observed in the present case as follows. A major flaw in the schematic displayed in Figure 2a is that it does not take into consideration the influence of the substrate lattice on the self-assembling pattern. It has been well documented in the literature that the substrate lattice has a strong bearing on the self-assembly of molecules.[14,61–63] The graphite lattice that is used as a substrate in the present study is built up of layers with a honeycomb arrangement of carbon atoms. The basal (001) plane of graphite has a threefold symmetry and the carbon atoms along the direction of any C_3 axis display the same zigzag extension as the zigzag skeleton of the carbon backbone of an all-*trans* alkyl chain. The in-plane lattice constant of 2.46 Å (the distance between two interval carbon atoms along any C_3 axis) is very close to every second neighbour carbon atom, 2.58 Å along the axis of an all-*trans* alkyl chain. This fortuitous match allows the methylene groups of an all-*trans* alkyl chain to rest over the voids of the hexagons of the graphite lattice,[63] thereby providing an approximately commensurate packing of the alkyl chains as displayed in Figure 3a. The lattice match between alkyl chains

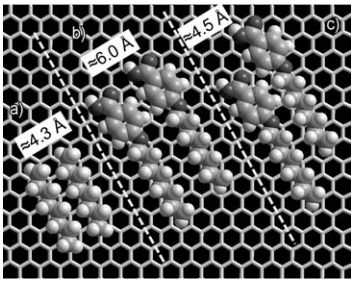

Figure 3. A molecular model depicting the packing of a) unsubstituted and two possible arrangements of b) phenyl-substituted (4-alkoxybenzoic acid in this case) and c) alkane derivatives on the surface of graphite. It is evident that the presence of a bulky head group in case of the latter prevents the close packing of the molecules in comparison with the corresponding unsubstituted alkane.

and the graphite substrate has been confirmed widely.[51,61–63] The lateral arrangement of alkyl chains on the graphite lattice is also governed by the similarity in the lattice parameters. Typically, it has been observed that the distance between unsubstituted alkanes within a lamella (along the lamella axis) is approximately 4.26 Å, which is in reasonable agreement with the distance between every other carbon row of the graphite lattice (4.24 Å). Thus the registry of the alkyl chains with the underlying graphite lattice requires that these chains should be placed close to (or in multiple integer of) 4.24 Å apart (Figure 3a). However, in the present case, the bulky phenyl head group attached to the alkoxy chain prevents the contentment of the alkyl-chain registry condition imposed by the graphite lattice. Thus, there is a competition between the restriction enforced by the substrate and the molecular packing parameter. If the alkoxybenzoic acid molecules are to be placed side-by-side on the surface of graphite, then they should be placed at least 6.0 Å apart as displayed in Figure 3b. However, as already mentioned, the registry mechanism demands a distance of 4.24 Å between two alkyl chains. Thus, the phenyl cores of the molecules are shifted with respect to each other such that the tails of the alkoxy chains are around 4.5 Å apart (Figure 3c). According to the Groszek model,[63] the lowest potential energy trough for the methylene units of an alkyl

chain is the centre of the hexagon of the graphite lattice with an interchain distance of 4.26 Å. Considering the experimentally observed distance of around 4.9 Å as well as the offset between adjacent phenyl rings, the alkyl chains of only three molecules can be placed with an approximate registry with the underlying graphite lattice in a given direction. The alkyl chain of the fourth molecule, however, does not follow the lattice registry correctly, with the methylene units located away from the centres of the graphite hexagons (see the Supporting Information). Thus, the aforementioned condition results in the accumulation of internal strain in the rows of molecules, which implies that it is energetically unfavourable to pack the molecules in straight rows along one given direction. Consequently, to follow the substrate lattice correctly, the fourth molecule is shifted in a direction that is different than the propagation direction of the previous three molecules. This shift allows the alkyl chain of the fourth molecule to register correctly with the underlying graphite lattice and hence the kinks appear after every three molecules. However, it must be noted that the conjecture proposed above is rather simplistic and other factors such as the length of the molecule as well as the interactions between the molecules from adjacent lamellae might also be responsible partially for the observed molecular arrangement. Besides this, the fact that 4-ABAs form a structurally different monolayer on the Au(111) surface[64] indirectly points towards the important role played by the graphite substrate on the self-assembly in the present case. Thus, the development of kinks or dislocations in the crystal lattice can be viewed as an intrinsic mechanism to relax the internal strain in the monolayer.

In addition to the registry mechanism proposed above, one can also consider the stabilisation of the molecular assembly by the formation of =C−H···O= hydrogen bonds between adjacent benzoic acid molecules. Such stabilisation appears to be sterically more feasible for the displaced arrangement depicted in Figure 2b than for the parallel arrangement in Figure 2a. The possibility of slight tilting of the phenyl rings to closely pack the molecules can also be considered. Such tilting of the phenyl rings might allow the alkoxy chains to follow the substrate lattice. However, the high-resolution image displayed in Figure 1b rules out this possibility because the bright features appear to be lying flat on the graphite surface. Moreover, the diameter of the bright spots ((0.69 ± 0.02) nm) matches well with the reported value for flat-lying isophthalic acid molecules on the surface of HOPG.[65]

The discussion presented in the previous paragraph illustrates that alkyl-chain registry and phenyl-group packing are the two critical and competing factors that govern the molecular ordering and are responsible for the emergence of kinked lamellae. So the obvious question is, "What happens if the alkyl-chain length is reduced?" To clarify this point further, a systematic study of 4-ABAs that possess shorter alkyl chains was undertaken wherein STM images of derivatives that possess alkoxy chains as short as butoxy were recorded. Figure 4 displays some of the representative STM

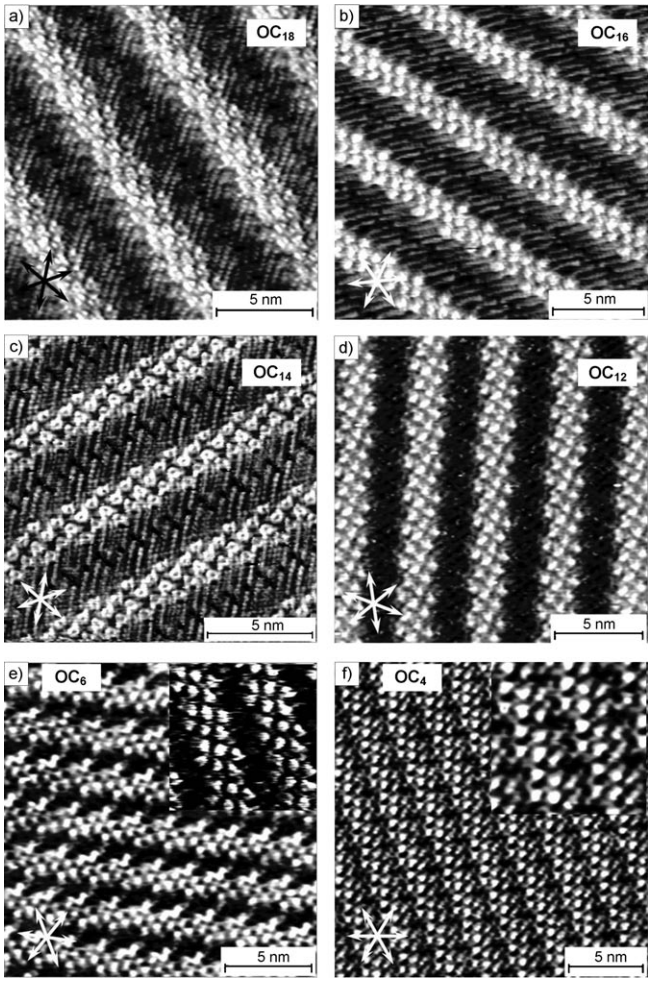

Figure 4. STM images of various 4-ABAs physisorbed at the 1-phenyloctane/HOPG interface. The number of carbon atoms in the alkoxy chain is indicated in each image. The inset in (e) and (f) shows the magnified area for the sake of clarity. It is evident from these images that a decrease in the alkoxy-chain length has no significant influence on the molecular arrangement except for a gradual decrease in the lamella width. Imaging conditions: $I_t = 0.31$ to 0.13 nA and $V_{bias} = 1.4$ to 0.65 V. (For STM images as well as unit-cell parameters of other derivatives, please see the Supporting Information).

images of 4-ABAs at the 1-phenyloctane–HOPG interface. It is clearly evident from the STM images that a decrease in the alkoxy-chain length has no significant influence on the packing of the acid molecules in the monolayer, apart from the gradual decrease in the lamella width. The kinks are present in the lamellar structure even for the shortest (4-butoxy) derivative investigated in this study. Thus, we can safely conclude that in case of 4-ABAs, a compromise between the registry mechanism imposed by the substrate and phenyl-group packing is largely responsible for the observed peculiar surface pattern.

Odd/even effects: During the systematic STM investigation of the 4-ABAs, it emerged that there is a slight difference in the packing of the derivatives that possess an even number of carbon atoms in the alkoxy chain compared to the ones

that have an odd number of carbon atoms. This has been observed for the derivatives that possess an alkyl-chain length of eight or fewer carbon atoms. Thus, the molecular packing in 4-heptyloxy (**4-OC$_7$BA**) and 4-pentyloxy (**4-OC$_5$BA**) derivatives is different than the corresponding tetra-, hexa- and octyloxy-substituted molecules. Figure 5 displays STM

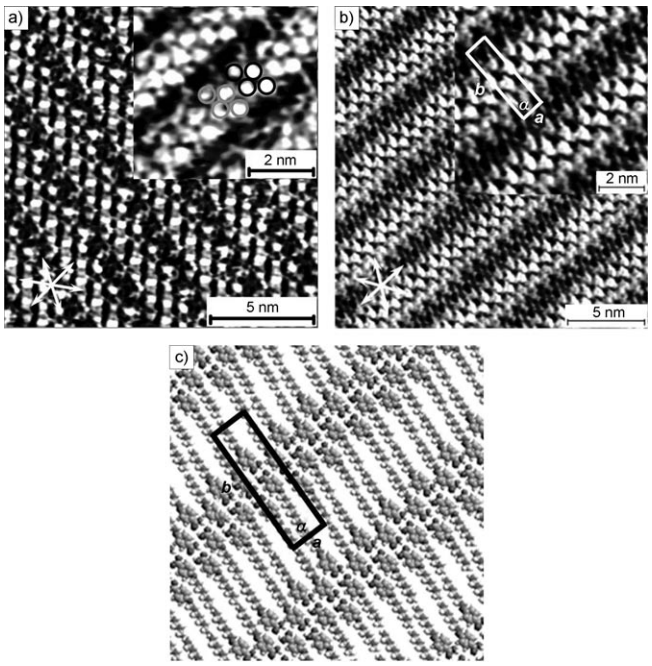

Figure 5. STM image of a) **4-OC$_5$BA** and b) **4-OC$_7$BA** physisorbed at the 1-phenyloctane–HOPG interface. Note that the kinks are present after every two dimers instead of three as observed for the derivatives that possess an even number of carbon atoms in the alkoxy chains. The unit-cell parameters are $a=(1.21\pm0.05)$ nm, $b=(2.72\pm0.08)$ nm and $\alpha=(88.3\pm1.5)°$ for **4-OC$_5$BA**; and $a=(1.18\pm0.04)$ nm, $b=(3.42\pm0.07)$ nm and $\alpha=(87.9\pm0.5)°$ for **4-OC$_7$BA** (plane group is $p2$). Imaging conditions: $I_t=0.15$ nA, $V_{bias}=-0.73$ V. c) Tentative model depicting the molecular arrangement in case of **4-OC$_7$BA**.

images of these derivatives at the 1-phenyloctane/HOPG interface. The STM images of **4-OC$_5$BA** (Figure 5a) and **4-OC$_7$BA** (Figure 5b) exhibit the dislocations in the lamella after every two dimers (every (1.2 ± 0.1) nm) instead of the normally observed difference of every three dimers (every (1.8 ± 0.1) nm). Thus, this dissimilar packing in case of the odd and even number of carbon-containing molecules gives rise to what has been termed as "microscopic odd/even effects" in the literature.[66] The odd/even effect is a widely observed phenomenon in chemistry, physics, biology as well as material science. It encompasses the differences in the structure and/or properties depending on the odd or even number of structural units in a molecule. Such odd/even effects observed in self-assembled organic monolayers have been found to influence many chemical, physical and interfacial properties such as chemical reactivity, electronic and electrochemical properties as well as friction behaviour.[66] In the present case, the number of carbon atoms serves as the odd/even unit. The appearance of odd/even effects in this system is an indication that the substrate registry has a strong influence on molecular ordering not only along the lamella propagation direction but also perpendicular to it. A similar phenomenon of emergence of odd/even effects in fractured lamellae has been observed earlier in case of alkylated cyanobiphenyls on the surface of MoS_2.[54,59,60] Lacaze et al.[67] have built a 2D phenomenological model and interpreted this phenomenon in terms of commensurate–incommensurate transition monitored by the molecular length. Odd/even effects are quenched, however, as we move to longer alkoxy chain derivatives as evident from the STM image displayed in Figure 6. 4-Heptadecyloxybenzoic acid

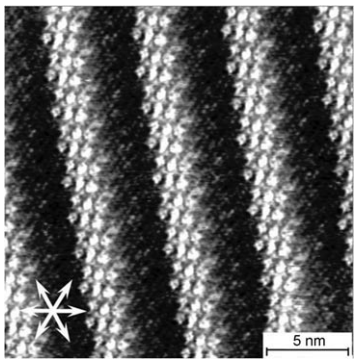

Figure 6. STM image of **4-OC$_{17}$BA** physisorbed at the 1-phenyloctane–HOPG interface. Note that the kinks are present after every three dimers instead of two as observed for the derivatives that possess an odd number of carbon atoms in the alkoxy chains. Thus the odd/even effect is quenched upon increasing the alkoxy-chain length. Imaging conditions: $I_t=0.12$ nA, $V_{bias}=-1.2$ V.

(**4-OC$_{17}$BA**) self-assembles in an identical pattern as that of its corresponding 4-octadecyloxy (**4-OC$_{18}$BA**) derivative. This is an indication that increased van der Waals interactions (molecule–molecule as well as molecule–substrate) with an increase in the alkoxy-chain length become more important than the odd/even difference and thus quench the odd/even effects in such a way that the molecular arrangement is identical for the odd and even molecules.

There are some discrepancies, however, if we look at the case of 4-nonyloxy (**4-OC$_9$BA**) and 4-undecyloxy (**4-OC$_{11}$BA**) benzoic acids. It was found that **4-OC$_9$BA** forms an entirely different pattern at the 1-phenyloctane–HOPG interface. Figure 7a shows the STM image of **4-OC$_9$BA** that is completely different from that observed for other derivatives in the series. Considering the similarity in molecular dimensions, one cannot rule out the possibility of co-adsorption of 1-phenyloctane[41] in this case. On the other hand, **4-OC$_{11}$BA** (Figure 7b) forms lamellae that are somewhat similar to the ones formed by the rest of the derivatives, the only difference being the lack of periodicity in the position of kinks along the lamella propagation direction. The location of kinks in this case is irregular. Having already seen that odd/even effects are quenched upon increasing the alkyl-chain length in the case of **4-OC$_{17}$BA**, we can speculate that **4-OC$_{11}$BA** can be a borderline case wherein the in-

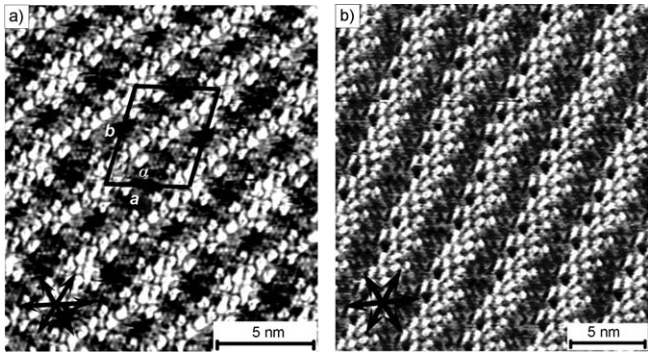

Figure 7. STM image of a) **4-OC$_9$BA** and b) **4-OC$_{11}$BA** physisorbed at the 1-phenyloctane–HOPG interface. Compound **4-OC$_9$BA** forms an entirely different pattern than the remaining homologues. A possibility of solvent co-adsorption cannot be ruled out in this case. Unit-cell parameters are as follows: $a=(4.13\pm0.06)$ nm, $b=(5.12\pm0.08)$ nm and $\alpha=(80.0\pm1.1)°$ (plane group is $p2$). The monolayer formed by **4-OC$_{11}$BA**, on the other hand, shows a bit of randomness in the appearance of kinks along the lamella axis. Imaging conditions: a) $I_t=0.2$ nA, $V_{bias}=-1.2$ V; b) $I_t=0.13$ nA, $V_{bias}=-0.9$ V.

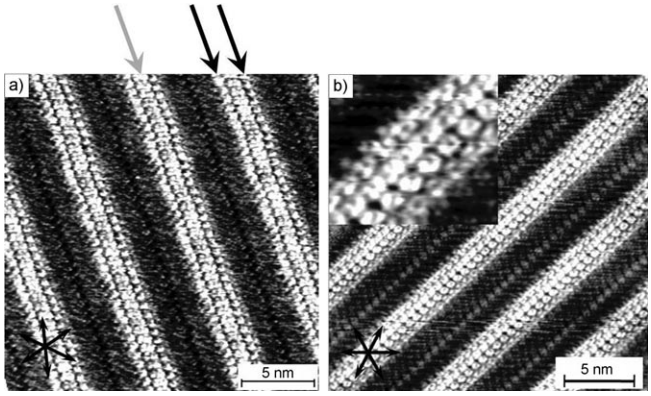

Figure 8. STM images of a) **4-OC$_{20}$BA** and b) **4-OC$_{18}$BA** complexed with 4,4′-bipyridine. The grey arrow in (a) indicates the location of bipyridine moieties, whereas the black arrows indicate the positions of phenyl rings of the benzoic acid molecules. The inset in (b) shows the corresponding high-resolution STM image. Note that the kinks are absent in this bicomponent system and the monolayer structure is continuous. Imaging conditions: a) $I_t=0.075$ nA, $V_{bias}=-0.85$ V; b) $I_t=0.095$ nA, $V_{bias}=-0.95$ V.

terchain van der Waals interactions start becoming more significant than the odd/even difference. It must be noted at this juncture that 4-decyloxy as well as 4-dodecyloxybenzoic acids show typical periodicity in the location of kinks along the lamella axis.

Complexation studies: To modulate the supramolecular pattern formed by 4-ABAs by manipulating the hydrogen-bonding interactions, complexation studies were undertaken. Furthermore, these experiments will also to help evaluate if the complexation reaction can be used to control the supramolecular patterns in such a way that all the benzoic acid derivatives form identical supramolecular patterns, thus leading to a structural convergence. To this effect, 4,4′-bipyridine, which acts as a hydrogen-bond acceptor, was used as a complexing agent. A saturated solution of 4,4′-bipyridine in 1-phenyloctane was added to a preformed monolayer of 4-ABA on the surface of HOPG. After allowing the system to equilibrate, STM images of the bicomponent monolayer were recorded. Figure 8 displays the STM images of **4-OC$_{20}$BA** and **4-OC$_{18}$BA** complexed with 4,4′-bipyridine. The central bright row in the lamellar structure corresponds to the bipyridine moieties, whereas the adjacent rows are the aromatic cores of the hydrogen-bonded benzoic acid molecules. The alkyl chains are not well resolved; nevertheless, there is sufficient indication that they are not interdigitated. The width of the lamella in case of **4-OC$_{20}$BA** is (5.8 ± 0.2) nm, whereas it is (5.4 ± 0.1) nm for the **4-OC$_{18}$BA** derivative. However, the most important feature of the STM images displayed in Figure 8 is the presence of continuous lamellar structure and complete disappearance of periodic dislocations that were prominent in the cases of the corresponding monocomponent systems. Thus, the aforementioned experiments illustrate that the incorporation of a hydrogen-bond-accepting agent in the 2D crystal lattice modulates the monolayer structure.

Complexation experiments carried out on the molecules that possess an odd number of carbon atoms in the alkoxy chain revealed an entirely different packing of the bicomponent system. Figure 9 gives representative STM images of 4,4′-bipyridine complexed with **4-OC$_{17}$BA**. The submolecularly resolved image displayed in Figure 9b clearly shows the microscopic features of the bicomponent monolayer. It is evident that the alkyl chains are nicely resolved, closely

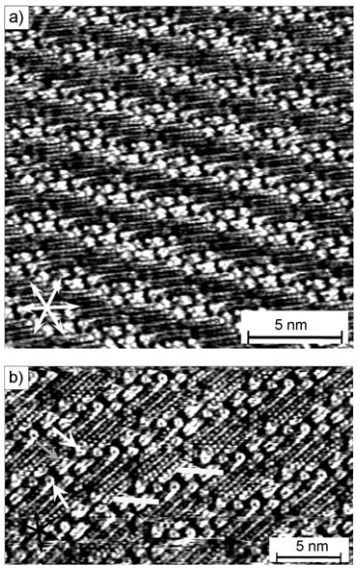

Figure 9. a) Complexation between **4-OC$_{17}$BA** and 4,4′-bipyridine at the 1-phenyloctane–HOPG interface. b) High-resolution STM image of the same system. The grey arrow in (b) indicates the location of the bipyridine moiety, whereas the white arrows show the positions of phenyl rings of the benzoic acid molecules. Note that the bipyridine moieties are not arranged in straight rows as is the case in Figure 8. The white bars are drawn as a visual aid to identify the offset in the molecular packing. Imaging conditions: a) $I_t=0.13$ nA, $V_{bias}=-1.2$ V; b) $I_t=0.13$ nA, $V_{bias}=-1.13$ V.

packed and interdigitated. The alkyl-chain interdigitation is in complete contrast to the bicomponent system of the corresponding **4-OC$_{18}$BA** and **4-OC$_{20}$BA** derivatives. Moreover, the bipyridine moieties are not arranged in straight rows. Instead, after every two bipyridine molecules, there is a shift in the propagation direction. Thus, in a sense, the kinks are still present in the lamellar structure. The white bars in Figure 9b are drawn for identifying the offset in the molecular packing. This peculiar molecular arrangement is surprising in view of the fact that **4-OC$_{17}$BA** does not show odd/even effect as already discussed in previous section. Thus, the odd/even difference that is insignificant in the monocomponent system appears to become prominent in the presence of the second component, which is the bipyridine unit in the present case. The outcome of complexation studies reveals that, although it is an effective way of modulating the self-assembly, it is not efficient enough to converge the structures of the various alkoxybenzoic acid derivatives on the surface, thus highlighting the importance of van der Waals interactions. These experiments, when extended to other molecules that possess an odd number of carbon atoms in the alkoxy chain (Figure S3 in the Supporting Information), reaffirm this point.

Similar experiments have been carried out in the recent past with an intent to tune 2D supramolecular patterns by adding an appropriate complexing agent to the self-assembled monolayer.[68–73] Qian et al.[68,69] have successfully employed 4,4′-bipyridine as a marker to study self-assembly[68] and chirality[69] in the monolayers formed by aliphatic fatty acids. Alkylated derivatives of 2,2′-bipyridine have been used as complexation scaffolds for metal-ion complexes. The use of such metal-ion complexes has been explored as a route to novel 2D templates.[8] Recently, Kikkawa et al.[70] have investigated the self-assembly and odd/even chain length effect in the case of various bipyridine derivatives. They could successfully induce a structural convergence in different 2D structures by using metal-ion complexation.[70] The outcome of the present investigation on complexation appears to be somewhat different than the previous reports in view of the fact that the odd/even effects remain prominent even in the bicomponent crystal lattice.

Solvent-induced structural convergence: For surface assemblies at the liquid–solid interface, solvent molecules play a vital role in the outcome of a given supramolecular pattern.[36–48] Apart from its chemical identity, typical solvent properties such as viscosity and polarity have an impact on the process of self-assembly. Various factors that contribute to the solvent dependence of self-assembly are solvent coadsorption, solvophilic/solvophobic effects, hydrogen-bonding and van der Waals interactions.[48] The delicate balance between all these factors makes it difficult to generalise the role of solvent in the process of 2D self-assembly. Thus, to comprehend the role of solvent in the formation of 2D supramolecular patterns in the case of 4-ABAs, we extended these investigations in 1-octanoic acid. 1-Octanoic acid is a structurally different solvent than 1-phenyloctane. It has a terminal carboxyl functional group that can be involved in hydrogen-bonding interactions with the solute molecules and hence may have an impact on the monolayer structure. In fact, hydrogen-bonding solvents have been known to play a significant role in the adsorbate monolayer structure.[74–77] Thus, in comparison with 1-phenyloctane, which is relatively a neutral partner in the self-assembly, 1-octanoic acid can indeed influence the molecular packing. Figure 10 gives a representative STM image of **4-OC$_{20}$BA** physisorbed at the 1-octanoic acid–HOPG interface. The bright spots that correspond to the phenyl rings are arranged in a zigzag fashion. The characteristic fractured molecular arrangement observed in 1-phenyloctane is absent. The width of the lamella is (4.11 ± 0.06) nm, which is smaller in comparison to that observed in 1-phenyloctane ((5.8 ± 0.1) nm) and is represented as ΔL in the image. The region of the lamella that lies in between the bright spots is not well resolved, though. Nevertheless, this STM image primarily illustrates that the molecular packing is entirely different in 1-octanoic acid than that observed in 1-phenyloctane. One of the surprising aspects of this monolayer structure is the presence of laterally placed bright features instead of head-on. In other words, based primarily on the molecular structure and substitution pattern, one expects these molecules to form hydrogen-bonded dimers and thus the bright features should appear opposite each other. Thus, the appearance and rationalisation of such features is an intriguing aspect and the role of 1-octanoic acid may hold a key in the development of such a peculiar structure.

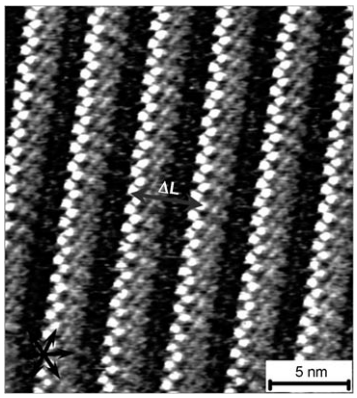

Figure 10. STM image of **4-OC$_{20}$BA** physisorbed at the 1-octanoic acid–HOPG interface. The width of the lamella is indicated as ΔL. Note that the structural pattern is entirely different than the one observed in 1-phenyloctane. The different contrast on either side of the bright spots is due to scanning artifacts. Imaging conditions: $I_t = 0.13$ nA, $V_{bias} = -1.2$ V.

With an intent to figure out the exact mode of interaction between solute and the solvent molecules, high-resolution STM images were recorded for this system. Figure 11 gives one such STM image that resolves the region between zigzag bright spots. It is evident that opposite every bright spot there lies one striped feature that can be attributed to the adsorbed molecule of 1-octanoic acid. The appearance

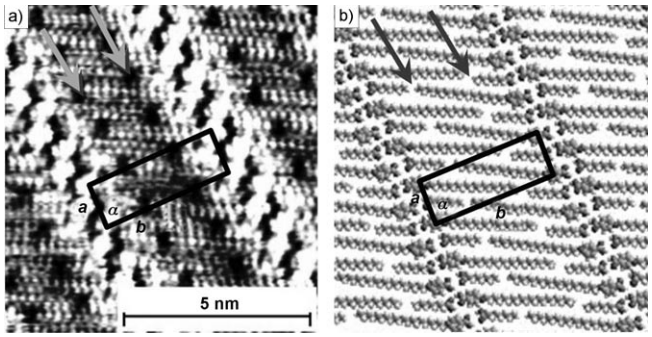

Figure 11. a) High-resolution STM image of **4-OC$_{20}$BA** physisorbed at the 1-octanoic acid–HOPG interface. Submolecularly resolved features indicate that 1-octanoic acid molecules are co-crystallised with benzoic acid molecules. b) Tentative model depicting the molecular arrangement. Arrows in (a) as well as (b) indicate the location of terminal methyl groups of constituent molecules. The region with darker contrast opposite each bright spot indicates the location of the hydrogen bonding between two molecules. Unit-cell parameters are as follows: $a=(1.24\pm0.03)$ nm, $b=(4.11\pm0.03)$ nm and $\alpha=(88.5\pm1.0)°$ (plane group $p2$). Imaging conditions: $I_t=0.13$ nA, $V_{bias}=-1.2$ V.

of a dark region opposite each bright spot can therefore be explained by the fact that the carboxyl functional groups do not appear in STM images.[61] The length of the striped feature opposite every bright spot ((1.1 ± 0.1) nm) is in good agreement with the length of 1-octanoic acid molecules (≈1.02 nm). Moreover, one can also decipher two rows of additional features that lie in between two zigzag rows of bright spots and within the striped features. These features correspond to the terminal methyl groups of 1-octanoic acid molecules, which are indicated by arrows in Figure 11.

From the discussion presented in the previous paragraph, it is clear that 1-octanoic acid molecules have a propensity to co-adsorb in view of their hydrogen-bonding ability. As a consequence of such hydrogen-bonding-induced co-adsorption phenomenon, a very small amount of solvent molecules actually become adsorbates and the rest of them remain in the continuous phase. Co-adsorption of solvent molecules can thus be considered as an alternative method to fabricate hybrid supramolecular patterns.[41] Similar co-adsorption behaviour has been reported by Bernasek et al.[76] when they investigated the self-assembly of 5-(octadecyloxy)isophthalic acid at the 1-octanoic acid–HOPG interface. They observed the formation of a molecular mesh as a result of insertion of octanoic acid molecules in the monolayer. We believe that, along with the co-adsorption phenomenon, the lateral hydrogen-bonding interactions between adjacent 5-(octadecyloxy)isophthalic acid molecules are equally significant in their experiments. In the present case, however, the only lateral interactions between adjacent molecules are the van der Waals interactions between the alkoxy chains. Moreover, we do not observe any pore formation as the molecules pack compactly without leaving any empty voids in the lamella. The fact that this two-component monolayer could be imaged with submolecular resolution demonstrates the excellent stability of this system. Perepichka et al.[29] have also observed co-adsorption of various aliphatic alcohols in the monolayer of TMA. The only difference in their case was that alcohols were added as solutes and heptanoic acid served as solvent.[29]

Having established the role of a hydrogen-bonding solvent in the process of self-assembly, it is imperative to verify if a similar effect can be induced in case of other 4-ABA molecules. More importantly, it would be intriguing to check if the solvent can be used as an internal agent to converge the structures. To this effect, STM images of a few representative 4-ABA derivatives were recorded in 1-octanoic acid. Figure 12a–d gives STM images of four different 4-ABA derivatives adsorbed at the 1-octanoic acid–HOPG interface. It can be easily noticed from these images that they all represent identical supramolecular pattern, thus giving ample evidence of structural convergence. However, it still remains

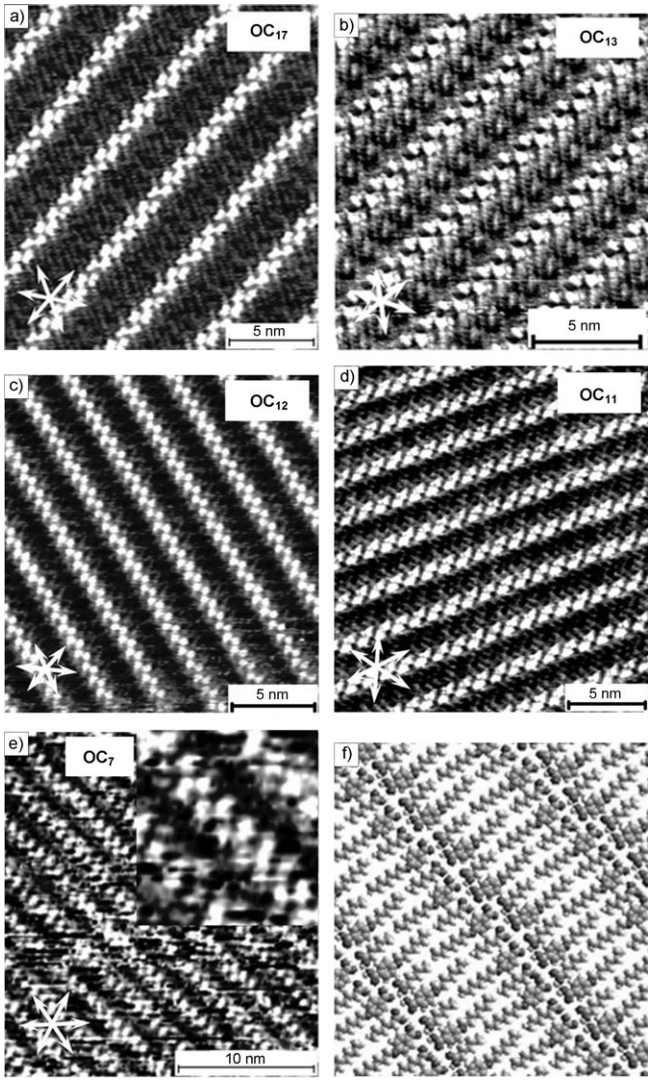

Figure 12. STM images of 4-ABAs a)–d) in 1-octanoic acid and e) in 1-hexanoic acid. The length of the alkoxy chain is indicated in each figure. It is evident that in the presence of a hydrogen-bonding solvent, the monolayers are converged into identical zigzag structures. The inset in (e) shows the magnified area for the sake of clarity. f) A tentative molecular model displaying molecular packing of **4-OC$_7$BA** in 1-hexanoic acid.

to be verified as to what happens to the lower members of 4-ABAs in 1-octanoic acid. The experiments aimed towards STM imaging of lower homologues in 1-octanoic acid were not fruitful. Preferential adsorption of the solvent molecules was observed instead of the solute molecules of interest. Thus, to prove that a hydrogen-bonding solvent can indeed bring about structural convergence, we carried out measurements in lower aliphatic acids. Figure 12e gives a representative case of **4-OC$_7$BA** physisosorbed at the 1-hexanoic acid–HOPG interface. Typical zigzag bright features can be discerned in this STM image, which clearly validate the structural convergence brought about by the solvent molecules.

Co-adsorption-induced structural convergence: Universal phenomenon or a specific case for 1-octanoic acid? The discussion presented in the previous paragraph suggests that presence of a hydrogen-bonding solvent molecule can modulate the monolayer structure through co-adsorption, thereby inducing structural convergence. It needs to be established whether this aspect is universal or specific for the case of 1-octanoic acid. Moreover, such a solvent co-adsorption phenomenon will allow us to test the competitive influence of hydrogen-bonding and van der Waals interactions at the level of the solvent. As already mentioned, the understanding of solvent effects in the process of 2D self-assembly is still in its infancy. Thus, to establish the parameters that govern the solvent co-adsorption phenomenon in the case of 4-ABAs, the following control experiments were carried out. First, the self-assembly of **4-OC$_{20}$BA** was attempted in 1-octanol, which is also capable of hydrogen bonding with the solute molecules. This molecule possesses a hydroxyl functional group instead of carboxyl and has identical molecular dimensions as that of 1-octanoic acid (effectively, the only difference being the absence of a carbonyl group). However, the molecular packing observed in this solvent (Figure S5 in the Supporting Information) is exactly the same as the one observed in case of 1-phenyloctane, thereby indicating that 1-octanol does not undergo co-adsorption with solute molecules. Thus, it appears that a solvent molecule that can form complementary hydrogen bonds is more favoured for co-adsorption than the one that can form only a single hydrogen bond. It can be argued that the effect of concentration might come into play in this case. At relatively high concentration, the benzoic acid molecules will 'find' each other more easily than molecules of solvent and hence solvent co-adsorption will not be favoured. However, it must be noted here that the concentration of benzoic acid was maintained at almost identical levels in the experiments that involved 1-octanoic acid as well as 1-octanol. Moreover, no pattern change was observed when similar experiments were carried out at a concentration that was two orders of magnitude lower ($\approx 10^{-6}$ M). It is worthwhile to consider results by Wan et al.[77,78] in terms of concentration effects on the solvent co-adsorption phenomenon. They recently reported the solvent dependence of the 2D self-assembly of a 5-(benzyloxy)isophthalic acid derivative.[77] According to their investigations, a solvent can contribute in the 2D self-assembly process either as a neutral (dispersant) or as an active (counterpart) partner. 1-Phenyloctane was found to behave as a relatively neutral partner, mainly contributing as a dispersion medium for the solute molecules. On the other hand, 1-octanoic acid and 1,2,4-trichlorobenzene were found to act as counterparts in the 2D lattice through co-adsorption with solute molecules.[78] The behaviour of 1-phenyloctane and 1-octanoic acid observed in the present study is somewhat in line with the results of Wan et al.[77] Concentration dependence on the solvent co-adsorption phenomenon was also investigated. It was observed that solvent co-adsorption is favoured at lower solute concentration.[78]

While considering the co-adsorption phenomenon of alkylated molecules, one cannot discount the role of interchain van der Waals interactions. To evaluate the influence of these interactions on the co-adsorption phenomenon, a second set of STM experiments was performed on **4-OC$_{20}$BA** and **4-OC$_7$BA** adsorbed at the butyric acid–HOPG interface. The justification for using this particular solvent is as follows. Butyric acid can also form complementary hydrogen bonds with benzoic acid molecules in an identical fashion to that of 1-octanoic acid. However, the shorter alkyl chain of the solvent will lead to decreased van der Waals interactions (both solute–solvent as well as solvent–substrate), thus allowing us to compare the competitive influence of complementary hydrogen-bonding and van der Waals interactions on the process of co-adsorption. However, it was observed that, despite having the capability to form complementary hydrogen bonds with the solute molecules, the co-adsorption of butyric acid molecules is not favoured in case of both the solutes, plausibly in view of insufficient van der Waals interactions. The molecular packing in butyric acid is exactly the same as the one observed in 1-phenyloctane (Figure S6 in the Supporting Information). Thus, on the basis of the control experiments described above, we can safely conclude that the co-adsorption phenomenon is governed by both hydrogen-bonding as well as van der Waals interactions and solvent co-adsorption is observed only when there is a perfect balance between these two interactions.[79]

Conclusion

It is difficult to predict the outcome of a supramolecular pattern on the basis of the chemical structure of the building blocks due to the crucial role played by noncovalent interactions. A better understanding of such interactions will lead to the improved ability to envisage and control the fate of surface-supported supramolecular patterns, which will in turn be valuable to program newer functional surfaces. We have systematically explored the competitive influence of two such noncovalent interactions, namely, hydrogen-bonding and van der Waals interactions, on the self-assembly of 4-alkoxybenzoic acids. The present study demonstrates that intermolecular hydrogen-bonding and interchain as well as molecule–substrate interactions (dominated by van der

Waals interactions) direct the molecules to form a peculiar self-assembled pattern with periodic dislocations in the crystal lattice. A closer look at the molecular structure and substrate lattice reveals that a competition between phenyl-group packing and alkyl-chain registry with the substrate is responsible for the development of periodic dislocations in the lamellae. These regular dislocations serve as an intrinsic mechanism to relieve the strain developed in the monolayer as a consequence of incommensurability with the underlying substrate. A systematic study on various 4-ABAs revealed that the periodicity of the kinks along the lamella axis depends on the number of carbon atoms in the alkoxy chain, thereby giving rise to microscopic odd/even effects prominent in the case of shorter alkoxy derivatives. The odd/even effect tends to vanish with increasing alkoxy-chain length. The emergence of odd/even effects further confirms the importance of van der Waals interactions (both interchain and molecule–substrate) in the 2D self-assembly. Insertion of a complexing agent that acts as a hydrogen-bond acceptor alters the supramolecular patterns. However, the complexation reaction fails to induce a structural convergence. The odd/even effects as well as kinked lamellae disappear when the molecules self-assemble at 1-octanoic acid–HOPG interface instead of 1-phenyloctane–HOPG interface. Thus, the solvent plays a significant role by being able to interact specifically with the solute molecules through complementary hydrogen-bonding interactions. High-resolution STM images illustrate that the solvent-induced structural convergence is effected by the coadsorption of solvent molecules in the 2D crystal lattice. The solvent-induced polymorphism probed by using solvents possessing different hydrogen bonding ability and alkyl chain lengths reveals that a perfect balance of these two factors is necessary so that the solvent molecules can undergo coadsorption.

Experimental Section

Materials and methods: All experiments were performed at room temperature (20–22 °C) using a PicoSPM (Agilent) operating in constant-current mode with the tip immersed in the supernatant liquid. STM tips were prepared by mechanical cutting from Pt/Ir wire (80%:20%, diameter 0.2 mm). Prior to imaging, the 4-alkoxybenzoic acid molecules were dissolved (concentration = 10^{-3} M to 10^{-4} M) in requisite solvents and a drop of this solution was applied onto a freshly cleaved surface of highly oriented pyrolytic graphite (HOPG, grade ZYB, Advanced Ceramics Inc., Cleveland, USA). The solvents used were 1-phenyloctane (Aldrich, 98%), 1-octanoic acid (Sigma, 99%), 1-hexanoic acid (Acros Organics 98%), butyric acid (Acros Organics 99%), 1-octanol (Sigma–Aldrich 99%) and tetradecane (99% Acros Organics). 4,4′-Bipyridine was obtained from Aldrich (98%) and was used without further purification. All complexation reactions were performed in situ. Thus, a drop of saturated solution of 4,4′-bipyridine in 1-phenyloctane was applied to a preformed monolayer of benzoic acid on the surface of HOPG. The experiments were repeated in several sessions using different tips to check for reproducibility and to avoid experimental artefacts, if any. For analysis purposes, recording of a monolayer image was followed by imaging the graphite substrate underneath it under the same experimental conditions, except for lowering the bias. The images were corrected for drift by using Scanning Probe Image Processor (SPIP) software (Image Metrology ApS), using the recorded graphite images for calibration purposes, thereby allowing a more accurate unit-cell determination. The unit-cell parameters were determined by examining at least 10 images and only the average values are reported. After the determination of the unit cell from the acquired STM images, a molecular model of the observed monolayer was constructed using the HyperChem program. First, a molecular model for a single molecule was built, and then this model was duplicated. The model of the entire monolayer was constructed by placing the molecules in accordance with the intermolecular distances and angles obtained from the analysis of the calibrated STM images. The imaging parameters are indicated in the figure captions: tunnelling current (I_t), and sample bias (V_t).

For the synthesis of the 4-alkoxybenzoic acids that were employed in this study, please see the Supporting Information.

Acknowledgements

This work is supported by the Fund of Scientific Research-Flanders (FWO), K. U. Leuven (GOA 2006/2), the Belgian Federal Science Policy Office (IAP-6/2) and the Institute of Nanoscale Physics and Chemistry (INPAC). K.S.M. thanks INPAC for a visiting postdoctoral fellowship and K.L. thanks the IWT-Flanders for financial support.

[1] *Comprehensive Supramolecular Chemistry, Vol. 6*, (Eds.: J. L. Atwood, J. E. D. Davies, D. D. MacNicol, F. Vögtle), Pergamon Press, New York, **1996**.
[2] J.-M. Lehn, *Proc. Natl. Acad. Sci. USA* **2002**, *99*, 4763–4768.
[3] G. M. Whitesides, M. Boncheva, *Proc. Natl. Acad. Sci. USA* **2002**, *99*, 4769–4774.
[4] A. Semenov, J. P. Spatz, M. Möller, J.-M. Lehn, B. Sell, D. Schubert, C. H. Weidl, U. S. Schubert, *Angew. Chem.* **1999**, *111*, 2701–2705; *Angew. Chem. Int. Ed.* **1999**, *38*, 2547–2550.
[5] J. V. Barth, J. Weckesser, C. Cai, P. Günter, L. Bürgi, O. Jeandupeux, K. Kern, *Angew. Chem.* **2000**, *112*, 1285–1288; *Angew. Chem. Int. Ed.* **2000**, *39*, 1230–1234.
[6] K. W. Hipps, L. Scudiero, D. E. Barlow, M. P. Cooke, Jr., *J. Am. Chem. Soc.* **2002**, *124*, 2126–2127.
[7] G. B. Pan, J.-M. Liu, H.–M. Zhang, L.-J. Wan, Q.-Y. Zheng, C.-L Bai, *Angew. Chem.* **2003**, *115*, 2853–2857; *Angew. Chem. Int. Ed.* **2003**, *42*, 2747.
[8] S. De Feyter, M. M. S. Abdel-Mottaleb, N. Schuurmans, J. V. Verkuijl, J. H. van Esch, B. L. Feringa, F. C. De Schryver, *Chem. Eur. J.* **2004**, *10*, 1124–1132.
[9] Y. Liu, L. Mu, B. Liu, J. Kong, *Chem. Eur. J.* **2005**, *11*, 2622–2631.
[10] D.-G. Choi, S. Kim, E. Lee, S.-M. Yang, *J. Am. Chem. Soc.* **2005**, *127*, 1636–1637.
[11] M. Lackinger, S. Griessl, W. Heckl, M. Hietschold, G. W. Flynn, *Langmuir* **2005**, *21*, 4984–4988.
[12] J. V. Barth, G. Costantini, K. Kern, *Nature* **2005**, *437*, 671–679.
[13] M. Ruben, *Angew. Chem.* **2005**, *117*, 1620–1623; *Angew. Chem. Int. Ed.* **2005**, *44*, 1594–1596.
[14] J. A. A. W. Elemans, S. De Feyter, *Soft Matter* **2009**, *5*, 721–735 and references therein.
[15] T. Kudernac, S. Lei, J. A. A. W. Elemans, S. De Feyter, *Chem. Soc. Rev.* **2009**, *38*, 402–421 and references therein.
[16] L. Piot, C. Marie, X. Feng, K. Müllen, D. Fichou, *Adv. Mater.* **2008**, *20*, 3854–3858.
[17] J. M. Mativetsky, M. Kastler, R. C. Savage, D. Gentilini, M. Palma, W. Pisula, K. Müllen, P. Samorì, *Adv. Funct. Mater.* **2009**, *19*, 2486–2494.
[18] A. Cnossen, D. Pijper, T. Kudernac, M. M. Pollard, N. Katsonis, B. L. Feringa, *Chem. Eur. J.* **2009**, *15*, 2768–2772.
[19] A. G. Phillips, L. M. A. Perdigao, P. H. Beton, N. R. Champness, *Chem. Commun.* **2010**, *46*, 2775–2777.
[20] K. Müllen, J. P. Rabe, *Acc. Chem. Res.* **2008**, *41*, 511–520.
[21] S. Chiang, *Chem. Rev.* **1997**, *97*, 1083–1096.

[22] S De Feyter, F. C. De Schryver, *J. Phys. Chem. B* **2005**, *109*, 4290–4302.
[23] A. Ulman, *Chem. Rev.* **1996**, *96*, 1533–1554 and references therein.
[24] M. Lackinger, S. Griessl, T. Markert, F. Jamitzky, W. M. Heckl, *J. Phys. Chem. B* **2004**, *108*, 13652–13655.
[25] A. Dmitriev, N. Lin, J. Weckesser, J. V. Barth, K. Kern, *J. Phys. Chem. B* **2002**, *106*, 6907–6912.
[26] S. Griessl, M. Lackinger, M. Edelwirth, M. Hietschold, W. M. Heckl, *Single Mol.* **2002**, *3*, 25–31.
[27] S. J. H. Griessl, M. Lackinger, F. Jamitzky, T. Markert, M. Hietschold, W. M. Heckl, *J. Phys. Chem. B* **2004**, *108*, 11556–11560.
[28] S. J. H. Griessl, M. Lackinger, F. Jamitzky, T. Markert, M. Hietschold, W. M. Heckl, *Langmuir* **2004**, *20*, 9403–9407.
[29] K. G. Nath, O. Ivasenko, J. A. Miwa, H. Dang, J. D. Wuest, A. Nanci, D. F. Perepichka, F. Rosei, *J. Am. Chem. Soc.* **2006**, *128*, 4212–4213.
[30] S. Lei, K. Tahara, F. C. De Schryver, M. Van der Auweraer, Y. Tobe, S. De Feyter, *Angew. Chem.* **2008**, *120*, 3006–3010; *Angew. Chem. Int. Ed.* **2008**, *47*, 2964–2968.
[31] T. Neuheuser, B. A. Hess, C. Reutel, E. Weber, *J. Phys. Chem.* **1994**, *98*, 6459–6467.
[32] G. Vidali, G. Ihm, H.-Y. Kim, M. W. Cole, *Surf. Sci. Rep.* **1991**, *12*, 135.
[33] S. Yin, C. Wang, X. Qiu, B. Xu, C. Bai, *Surf. Interface Anal.* **2001**, *32*, 248–252.
[34] S. De Feyter, A. Gesquière, M. Klapper, K. Müllen, F. C. De Schryver, *Nano Lett.* **2003**, *3*, 1485–1488.
[35] S. De Feyter, A. Gesquière, M. M. Abdel-Mottaleb, P. C. M. Grim, F. C. De Schryver, C. Meiners, M. Sieffert, S. Valiyaveetyil, K. Müllen, *Acc. Chem. Res.* **2000**, *33*, 520–531.
[36] B. Venkataraman, J. J. Breen, G. W. Flynn, *J. Phys. Chem.* **1995**, *99*, 6608–6619.
[37] P. Vanoppen, P. C. M. Grim, M. Rücker, S. De Feyter, G. Moessner, S. Valiyaveetil, K. Müllen, F. C. De Schryver, *J. Phys. Chem.* **1996**, *100*, 19636–19641.
[38] D. G. Yablon, D. Wintgens, G. W. Flynn, *J. Phys. Chem. B* **2002**, *106*, 5470–5475.
[39] C.-J. Li, Q.-D. Zeng, C. Wang, L.-J. Wan, S.-L. Xu, C.-R. Wang, C.-L. Bai, *J. Phys. Chem. B* **2003**, *107*, 747–750.
[40] W. Mamdouh, H. Uji-i, A. E. Dulcey, V. Percec, S. De Feyter, F. C. De Schryver, *Langmuir* **2004**, *20*, 7678–7685.
[41] W. Mamdouh, H. Uji-i, J. S. Ladislaw, A. E. Dulcey, V. Percec, F. C. De Schryver, S. De Feyter, *J. Am. Chem. Soc.* **2006**, *128*, 317–325.
[42] K. Tahara, S. Furukawa, H. Uji-i, T. Uchino, T. Ichikawa, J. Zhang, W. Mamdouh, M. Sonoda, F. C. De Schryver, S. De Feyter, Y. Tobe, *J. Am. Chem. Soc.* **2006**, *128*, 16613–16625.
[43] H. Xu, A. Minoia, Z. Tomovic, R. Lazzaroni, E. W. Meijer, A. P. H. J. Schenning, S. De Feyter, *ACS Nano* **2009**, *3*, 1016–1024.
[44] L. Kampschulte, M. Lackinger, A.–K. Maier, R. S. K. Kishore, S. Griessl, M. Schmittel, W. M. Heckl, *J. Phys. Chem. B* **2006**, *110*, 10829–10836.
[45] X. Shao, X. Luo, X. Hu, K. Wu, *J. Phys. Chem. B* **2006**, *110*, 1288–1293.
[46] Y. B. Li, G. C. Qi, Y. L. Yang, Q. D. Zeng, X. L. Fan, C. Wang, *J. Phys. Chem. C* **2008**, *112*, 8649–8653.
[47] F. Tao, S. L. Bernasek, *Langmuir* **2007**, *23*, 3513–3522.
[48] Y. Yang, C. Wang, *Curr. Opin. Colloid Interface Sci.* **2009**, *14*, 135–147 and references therein.
[49] S. Ahn, C. N. Morrison, A. J. Matzger, *J. Am. Chem. Soc.* **2009**, *131*, 7946–7947.
[50] They also differ by their pK_a. Benzoic acid: pK_a = 4.19; isophthalic acid: pK_a = 3.54, 4.60; terephthalic acid: pK_a = 3.51, 4.82; *CRC Handbook of Chemistry and Physics*, 55th edition (Ed.: R. C. Weast), CRC Press, **1974**–1**975**.
[51] B. Ilan, G. M. Florio, M. S. Hybertsen, B. J. Berne, G. W. Flynn, *Nano Lett.* **2008**, *8*, 3160–3165.
[52] J. Foster, J. E. Frommer, *Nature* **1988**, *333*, 542–545.
[53] D. P. E. Smith, J. K. H. Hörber, C. Gerber, G. Binnig, *Science* **1989**, *245*, 43–45.
[54] M. Hara, Y. Iwakabe, K. Tochigi, H. Sasabe, A. F. Garito, A. Yamada, *Nature* **1990**, *344*, 228–230.
[55] D. P. E. Smith, J. K. H. Hörber, G. Binnig, H. Nejoh, *Nature* **1990**, *344*, 641–644.
[56] T. J. McMaster, H. Carr, M. J. Miles, P. Cairns, V. J. Morris, *J. Vac. Sci. Technol. A* **1990**, *8*, 672–674.
[57] H. Nejoh, D. P. E. Smith, M. Aono, *Nanotechnology* **1991**, *2*, 214–220.
[58] T. Kadotani, S. Taki, H. Okabe, S. Kai, *Jpn. J. Appl. Phys.* **1996**, *35*, L1345–L1347.
[59] S. Taki, T. Kadatoni, S. Kai, *J. Phys. Soc. Jpn.* **1999**, *68*, 1286–1291.
[60] S. Taki, H. Okabe, S. Kai, *Jpn. J. Appl. Phys., Part 1* **2003**, *42*, 7053–7056.
[61] D. M. Cyr, B. Venkataraman, G. W. Flynn, *Chem. Mater.* **1996**, *8*, 1600–1615.
[62] C. Arrigoni, G. Schull, D. Bléger, L. Douillard, C. Fiorini-Debuischert, F. Mathevet, D. Kreher, A.-J. Attias, F. Charra, *J. Phys. Chem. Lett.* **2010**, *1*, 190–194.
[63] A. J. Groszek, *Proc. R. Soc. London Ser. A* **1970**, *314*, 473–498.
[64] N. Katsonis (private communication).
[65] S. Lei, M. Surin, K. Tahara, J. Adisoejoso, R. Lazzaroni, Y. Tobe, S. De Feyter, *Nano Lett.* **2008**, *8*, 2541.
[66] F. Tao, S. L. Bernasek, *Chem. Rev.* **2007**, *107*, 1408–1453 and references therein.
[67] E. Lacaze, P. Barois, R. Lacaze, *J. Phys. I France* **1997**, *7*, 1645–1664.
[68] P. Qian, H. Nanjo, T. Yokoyama, T. M. Suzuki, *Chem. Commun.* **1999**, 1197–1198.
[69] P. Qian, H. Nanjo, T. Yokoyama, T. M. Suzuki, K. Akasakab, H. Orhui, *Chem. Commun.* **2000**, 2021–2022.
[70] Y. Kikkawa, E. Koyama, S. Tsuzuki, K. Fujiwara, K. Miyake, H. Tokuhisa M. Kanesato, *Chem. Commun.* **2007**, 1343–1345.
[71] D. G. Kurth, N. Severin, J. P. Rabe, *Angew. Chem.* **2002**, *114*, 3833–3835; *Angew. Chem. Int. Ed.* **2002**, *41*, 3681–3683.
[72] A. Dmitriev, H. Spillmann, N. Lin, J. V. Barth, K. Kern, *Angew. Chem.* **2003**, *115*, 2774; *Angew. Chem. Int. Ed.* **2003**, *42*, 2670—2673.
[73] W. Mamdouh, M. Dong, S. Xu, E. Rauls, F. Besenbacher, *J. Am. Chem. Soc.* **2006**, *128*, 13305–13311.
[74] B. J. Gyarfas, B. Wiggins, M. Zosel, K. W. Hipps, *Langmuir* **2005**, *21*, 919–923.
[75] W. A. English, K. W. Hipps, *J. Phys. Chem. C* **2008**, *112*, 2026–2031.
[76] F. Tao, S. L. Bernasek, *J. Am. Chem. Soc.* **2005**, *127*, 12750–12751.
[77] X. Zhang, Q. Chen, G.-J. Deng, Q.-H. Fan, L.-J. Wan, *J. Phys. Chem. C* **2009**, *113*, 16193–16198.
[78] X. Zhang, T. Chen, Q. Chen, G.-J. Deng, Q.-H. Fan, L.-J. Wan, *Chem. Eur. J.* **2009**, *15*, 9669–9673.
[79] The self-assembly of 4-ABAs was also studied in tetradecane. The 2D patterns in tetradecane are identical to those formed in 1-phenyloctane. For STM data in tetradecane, please refer to Figure S7 in the Supporting Information.

Received: June 11, 2010
Published online: November 9, 2010

